

Reactions of hot deuterium atoms with OCS in the gas phase and in OCS-DI complexes

E. Böhmer, K. Mikhaylichenko, and C. Wittig

University of Southern California, Department of Chemistry, Los Angeles, California 90089-0482

(Received 2 April 1993; accepted 12 July 1993)

Reactions of photolytically prepared hot deuterium atoms with OCS have been investigated: (i) under gas phase, single collision, arrested relaxation (i.e., bulk) conditions; and (ii) by photoinitiating reactions within weakly bound OCS-DI complexes. Nascent SD($X^2\Pi$, $v=0$) rotational, spin-orbit, and Λ -doublet populations were obtained for the photolysis wavelengths 250, 225, and 223 nm by using $A^2\Sigma \leftarrow X^2\Pi$ laser induced fluorescence (LIF). The reason for using deuterium is strictly experimental: $A^2\Sigma$ predissociation rates are considerably smaller for SD than for SH. The SD ($v=0$) rotational distribution was found to be very cold and essentially the same for both bulk and complexed conditions; the most probable rotational energy is ~ 180 cm^{-1} . No bias in Λ -doublet populations was detected. Spin-orbit excitation for bulk conditions was estimated to be $[^2\Pi_{1/2}]/[^2\Pi_{3/2}] \sim 0.25$, where $^2\Pi_{1/2}$ is the upper spin-orbit component. This ratio could not be obtained with complexes because of limited S/N. The complete set of present and past experimental findings, combined with recent theoretical results of Rice, Cartland, and Chabalowski suggest a mechanism in which SD derives from a very short lived HSCO precursor. This can result from direct hydrogen attack at the sulfur and/or the transfer of hydrogen from carbon to sulfur via the HCOS intermediate.

INTRODUCTION

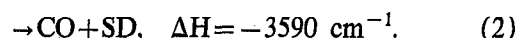
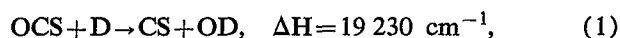
Studies of reactions of fast hydrogen atoms with triatomic molecules—both under gas phase, single collision, arrested relaxation (i.e., bulk) conditions, and photoinitiated within weakly bound complexes—have proven vehicular to furthering our understanding of chemical change in these prototypical systems. The past decade has witnessed a surge of activity in this area, as concentrated efforts, both experimental and theoretical, have addressed fundamental issues such as mechanism, stereospecificity, dynamics, statistics, etc. Much of this has paid off, and it now appears that a quantitative understanding may be within reach for at least some of these tetratomic systems. For example, studies of the important combustion reaction $\text{H}=\text{CO} \rightleftharpoons \text{HOCO} \rightleftharpoons \text{OH}+\text{CO}$ were carried out using weakly bound precursor complexes that are known to have qualitatively different ground state geometries, i.e., quasilinear $\text{CO}_2\text{-HCl}$ vs inertially T-shaped $\text{CO}_2\text{-HBr}$ and $\text{CO}_2\text{-HI}$.¹⁻¹⁸ These different structures enabled different hydrogen approaches to be examined, and the experiments revealed a remarkable degree of entrance channel regioselectivity, i.e., a large steric effect favoring broadside over end-on approaches. (We take the term “broadside” to include all possible sideways approaches, though only collisions at the oxygen site are reactive in the $\text{H}+\text{CO}_2$ system.) Such experiments provided insight into the entrance channel transition state.

The somewhat more complicated $\text{H}+\text{N}_2\text{O}$ system provides additional challenges.^{15-17,19-23} The presence of two chemically distinct product channels ($\text{OH}+\text{N}_2$ and $\text{NH}+\text{NO}$) brings up further questions of site specificity and mechanism under bulk conditions and in photoinitiated weakly bound complexes. For example, what are the respective roles of initial hydrogen attack at the terminal

nitrogen vs at the oxygen? From what is known about the potential energy surface (PES),¹⁹ one might think that product OH can be produced via two mechanisms: (i) direct attack at the oxygen; and (ii) initial attack at the nitrogen to form an HNNO^\ddagger intermediate, followed by hydrogen migration to the oxygen side. However, it was shown that under bulk conditions the indirect 1,3-hydrogen shift mechanism is responsible for at least the majority of the OH production.²³ How the environment presented by $\text{N}_2\text{O-HI}$ precursor complexes influences the mechanism awaits further scrutiny.

The $\text{H}+\text{CO}_2$ and $\text{H}+\text{N}_2\text{O}$ systems have inspired other experimental studies and have benefited from complementary theoretical work. On the other hand, the reaction of hot hydrogen atoms with OCS, which is isovalent with CO_2 , has received relatively little attention. Though it offers several important advantages over the $\text{H}+\text{N}_2\text{O}$ and $\text{H}+\text{CO}_2$ systems, such as two detectable product channels with the possibility of selectively accessing the higher energy channel by using complexes, experimental work has been relatively limited and only recently has theoretical work become available to help discern reaction mechanisms.^{24,25}

In this paper, we report nascent SD ($X^2\Pi$) rotational, spin-orbit, and Λ -doublet populations obtained for the photolysis wavelengths 250, 225, and 223 nm under bulk conditions and with complexes. The reason for using deuterium is strictly experimental; detection is easier for SD than SH, as discussed below. In the reaction with OCS, there are two distinct product channels which have been observed by other groups as well as in our laboratory;²⁵⁻³⁰



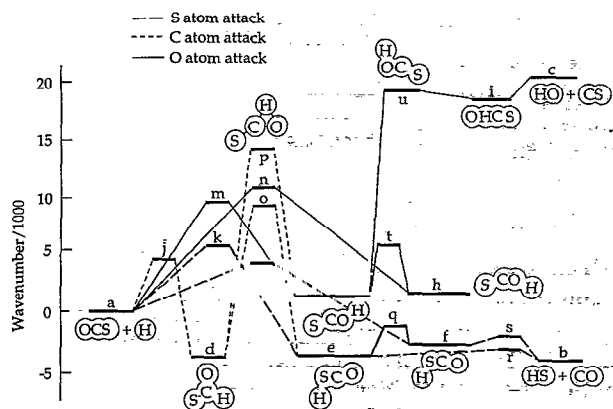


FIG. 1. Energy level diagram for the $\text{H}+\text{OCS}$ potential energy surface showing the minima and saddle point energies calculated at the PUMP4/PUMP2/6-31G** level (Ref. 24). Relative energies are given in cm^{-1} .

Figure 1 shows an energy diagram for the $\text{H}+\text{OCS}$ system.²⁴ The values used for the construction of this diagram are those calculated by Rice, Cartland, and Chabalowski, and are given in Table I.²⁴ Under bulk conditions, the hydrogen atom can attack at three different sites; (i) the S end, forming HSCO, (ii) the central C atom, forming HCOS, and (iii) the O end, forming HOCS. Hydrogen atoms attacking the sulfur end face entrance channel barriers of $\sim 4000 \text{ cm}^{-1}$ and $\sim 5500 \text{ cm}^{-1}$ leading to *cis*-HSCO and *trans*-HSCO, respectively. Once past the entrance channel barrier, HS-CO bond cleavage occurs without the involvement of a long lived intermediate, leaving no time for randomization of internal energy. Hydrogen attack at the central carbon proceeds over an entrance barrier which is comparable to that for sulfur atom attack and leads to the formation of a relatively stable HCOS intermediate.²⁴ For the reaction to proceed further to

trans-HSCO or *trans*-HOCS, barriers of $\sim 9000 \text{ cm}^{-1}$ and $\sim 14000 \text{ cm}^{-1}$, respectively, must be overcome which makes exiting via the entrance channel a more likely process. Nonetheless, since we are only sensitive to products, the HCOS intermediate can be a viable source of SD and OD. Finally, hydrogen attack at the oxygen can lead to $\text{OH}+\text{CS}$. There are entrance channel barriers of $\sim 10000 \text{ cm}^{-1}$ and $\sim 9300 \text{ cm}^{-1}$ leading to *cis*- and *trans*-HOCS, respectively. For *cis*-HOCS, no correlation to $\text{OH}+\text{CS}$ was found,²⁴ but *trans*-HOCS goes to $\text{OH}+\text{CS}$ with no barrier other than the reaction endothermicity.

Earlier experimental work on $\text{H}+\text{OCS}$ revealed a 300 K rate constant of $1.4 \times 10^{-14} \text{ cm}^3 \text{ molecule}^{-1} \text{ s}^{-1}$ and an activation energy of 1350 cm^{-1} . No attempt was made to infer the detailed reaction mechanism.^{27,28} Insight into the mechanism was gained experimentally through studies of the internal energies of the SD and OD products.³⁰ The SD rotational population obtained under bulk conditions was found to be nonstatistical (very cold), while the rotational population of the OD fragment could be fitted with a simple statistical model.³⁰ Häusler *et al.* pointed out that their data (taken under bulk conditions) could be reconciled by deuterium attack at the sulfur, yielding a short-lived intermediate for reaction (2).³⁰ However, the question of whether reaction favors broadside or end-on approaches could not be settled. The study reported here presents nascent SD rotational distributions obtained under bulk conditions and with complexes. The SD rotational distributions obtained with complexes may, in principle, reveal the attack direction, provided there is minimal interference from the nearby halogen atom.

The nascent CO product from reaction (2) has been studied under bulk conditions by Nickolaissen *et al.*, who found it to be rotationally and vibrationally colder than predicted on statistical grounds.²⁵ Consequently, they invoked end-on hydrogen attack at the sulfur. On the other hand, the amount of CO vibrational excitation could not be reconciled with a Franck-Condon analysis based on a sudden change of the CO bond length from that in OCS to that of free CO.²⁵ Specifically, this yielded less CO vibrational energy than was observed experimentally, suggesting that a small amount of energy is probably coupled into the CO stretch of the HSCO intermediate during reaction.

Important questions remain. Is migration, such as that involved in the $\text{H}+\text{N}_2\text{O}$ system, responsible for the amount of vibrational excitation found for CO? Is short-lived HSCO reached by direct attack or by migration? From an end-on approach or from a broadside approach? Are there mechanistic differences between bulk and complexed conditions?

We believe that a consistent picture can now be put forth based on; (i) all past and present experimental results; and (ii) recent theoretical studies.^{24,25}

EXPERIMENT

The experimental arrangement is shown schematically in Fig. 2. A full description has been given previously,²³ so only details germane to the current study are presented here. For 300 K bulk experiments, OCS and DI entered

TABLE I. Relative energies (cm^{-1}) of species on the $\text{H}+\text{OCS}$ potential energy surface at the configurations shown in Fig. 1 (taken from Ref. 24).

a	$\text{H}+\text{OCS}$	0
b	$\text{SH}+\text{CO}$	-4029
c	$\text{OH}+\text{CS}$	20 318
d	HCOS	-3781
e	<i>trans</i> -HSCO	-3620
f	<i>cis</i> -HSCO	-2665
g	<i>trans</i> -HOCS	1315
h	<i>cis</i> -HOCS	1581
i	$\text{OH}+\text{CS}$	18 418
j	$\text{H}+\text{OCS} \rightarrow \text{HOCS}$	4512
k	$\text{H}+\text{OCS} \rightarrow \text{trans-HSCO}$	5512
l	$\text{H}+\text{OCS} \rightarrow \text{cis-HSCO}$	4194
m	$\text{H}+\text{OCS} \rightarrow \text{trans-HOCS}$	9346
n	$\text{H}+\text{OCS} \rightarrow \text{cis-HOCS}$	10 161
o	$\text{HCOS} \rightarrow \text{trans-HSCO}$	9125
p	$\text{HCOS} \rightarrow \text{trans-HOCS}$	13 969
q	$\text{trans-HSCO} \rightarrow \text{cis-HSCO}$	-1126
r	$\text{trans-HSCO} \rightarrow \text{SH}+\text{CO}$	-2840
s	$\text{cis-HSCO} \rightarrow \text{SH}+\text{CO}$	-1927
t	$\text{trans-HOCS} \rightarrow \text{cis-HOCS}$	5701
u	$\text{trans-HOCS} \rightarrow \text{OH}+\text{CS}$	19 114

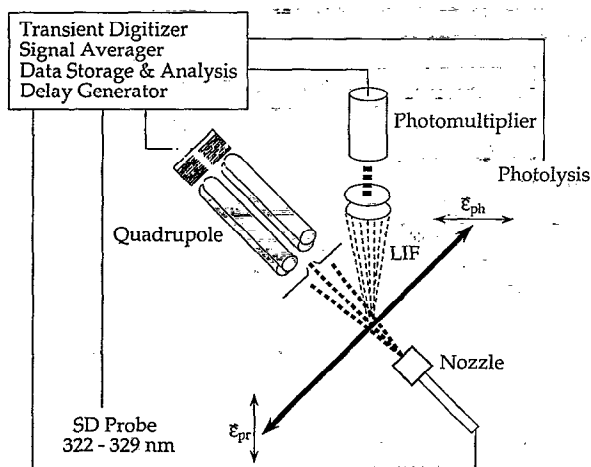


FIG. 2. Schematic drawing of the experimental arrangement.

the chamber through separate inlets. Reactions were then initiated in flowing samples of typically 50% OCS and 50% DI at 40 mTorr total chamber pressure. SD ($X^2\Pi$) nascent populations were obtained by using laser induced fluorescence (LIF); $A^2\Sigma \leftarrow X^2\Pi$ transitions were excited at wavelengths 322–330 nm. The delay between the excitation and probe lasers was 100 ns. As stated above, DI was preferred over HI for experimental convenience; SD ($A^2\Sigma$) predissociation rates are an order of magnitude smaller than those for SH, making SD more desirable for laser-induced fluorescence (LIF) studies.^{31–33} The predissociation lifetime of SD($A^2\Sigma^+$, $v=0$) was measured by Friedl *et al.* and was found to be 260 ± 100 ns.³² The change in predissociation lifetime with increasing rotational quantum number N was found to be small up to $N=10$.³² For the evaluation of our spectra, this was carefully taken into account.

The broad DI absorption spectrum allows the photolysis wavelength to be varied considerably by using the doubled output of an excimer-laser-pumped dye laser. DI was photolyzed at 250, 225, and 223 nm. Photodissociation of DI(DBr) yields both ground state $X(^2P_{3/2})$ and excited state $X(^2P_{1/2})$, where $X=I, Br$. Thus, D atoms are produced with two different kinetic energies. Though the kinetic energies corresponding to $X(^2P_{1/2})$ are insufficient to produce OD for any of the photolysis wavelengths, both slower and faster deuterium atoms contribute to SD production. The reported SD populations therefore reflect contributions from both D atoms for all photolysis wavelengths.

An important fact is that OCS and DI(DBr) can react heterogeneously to yield D_2S and/or other unwanted species. Therefore, simultaneous contact of OCS and DI(DBr) with surfaces should be minimized. In previous experiments with OCS–DI complexes,³⁰ OCS and DI were mixed in a cylinder prior to entering the nozzle. Unfortunately, it was not possible to eliminate heterogeneous processes completely by cleaning and/or coating the cylinder. For the present studies, an additional method was developed. DI was expanded through a pulsed nozzle

(0.25 mm diam) at backing pressures of 1000–1300 Torr and OCS was injected into this expansion with a separate cw expansion (0.2 mm diam, 500–800 Torr backing pressure) that is very close to—and merges with—the DI expansion. With this arrangement, the chamber pressure could be maintained at $\sim 10^{-4}$ Torr. For experiments with premixed samples, typical relative concentrations were 7% OCS, 2% DI, and 91% He. For the “merged-expansions” approach, mixtures of 7% OCS, 2%–5% DI, and 88%–91% He were used. Nozzle effluents were monitored with a mass spectrometer; about 20% of the cluster ion signals were higher than binary for both methods. Optimized OCS–DI⁺ signals were about five times weaker for the merged-expansion approach than for premixed samples. Reactions in higher-than-binary complexes do therefore contaminate the observed SD distributions to some degree, but we do not believe this will change the conclusions reported here. Nascent SD populations were observed 70 ns after photolysis. To ensure that SD product derived from complexes and not bimolecular reaction, signal amplitudes were monitored while the pump–probe delay was varied. No buildup time was observed.

RESULTS

(SD) LIF spectra were obtained under bulk conditions and with complexes; Fig. 3 shows representative parts of the spectra. Figure 3(b) is the first reported spectrum for SD obtained under complexed conditions for the reaction of hot D atoms with OCS. Signals were normalized for laser intensities, pressures (bulk conditions), and mass spectrometer signals (complexes). Transitions were assigned with a spectrum calculated from published molecular constants.^{34,35} Comparisons were made to the spectrum of Weiner *et al.*³⁶

Rotational level distributions (RLDs) for the $^2\Pi_{3/2}$ lower spin–orbit state were obtained from fits to the spectra. It was not possible to obtain RLDs for the $^2\Pi_{1/2}$ upper spin–orbit state because of low S/N. Figure 4 therefore shows only the $^2\Pi_{3/2}$ RLD (225 nm photolysis). Within the experimental uncertainty, no bias in the Λ -doublet populations was observed. This, as well as a bias favoring the lower spin–orbit state, agrees with earlier results.³⁰ Only an estimate can be given for the total $^2\Pi_{1/2}$ population relative to the total $^2\Pi_{3/2}$ population: $[^2\Pi_{1/2}]/[^2\Pi_{3/2}] \sim 0.25$. Comparison with the data of Häusler *et al.* suggests that this ratio increases with excess energy.³⁰

The RLD for 250 nm photolysis is decidedly nonstatistical, peaking at ~ 180 cm⁻¹; see Fig. 5. This is extremely cold considering that 18 170 cm⁻¹ is available for product excitations. RLDs obtained with 225 and 223 nm photolysis (corresponding to excess energies of 22 400 and 22 780 cm⁻¹, respectively) are essentially the same.

To ensure that the SD product observed with complexes does not derive from a D_2S contaminant, experiments were carried out in the two different ways mentioned above. In addition, DI was photolyzed at 250 nm to ensure that the small D_2S contamination present in the system is not the source of the observed SD. Spectra obtained with both methods are the same within experimental limits. Af-

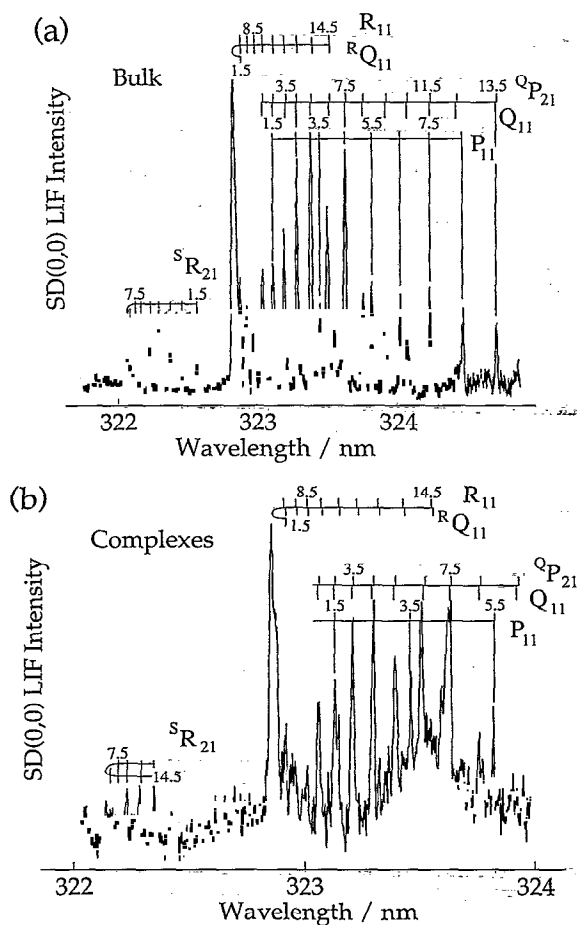
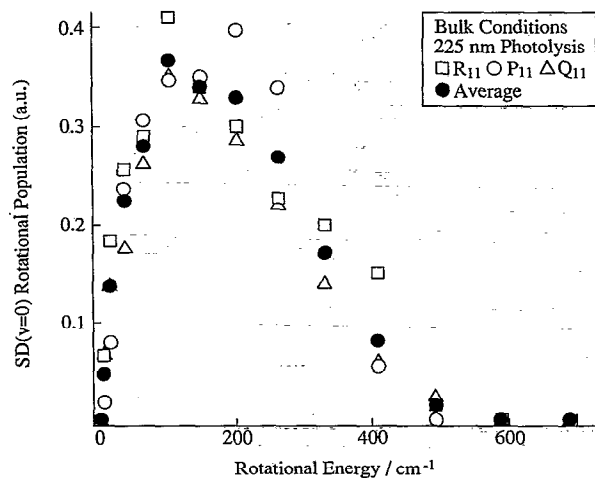


Figure 1 is a scatter plot showing the rotational energy dependence of the SD($v=0$) rotational population for bulk conditions at three different excitation wavelengths: 250 nm, 225 nm, and 223 nm. The y-axis represents the SD($v=0$) Rotational Population in arbitrary units (a.u.), ranging from 0 to 0.35. The x-axis represents the Rotational Energy in cm^{-1} , ranging from 0 to 600. The legend indicates that open circles represent 250 nm, filled circles represent 225 nm, and open squares represent 223 nm. The data shows that the rotational population is highest at low rotational energies (below 100 cm^{-1}) and generally decreases as rotational energy increases, with some fluctuations. The 225 nm and 223 nm conditions show higher populations at higher rotational energies compared to the 250 nm condition.

Rotational Energy / cm^{-1}	SD($v=0$) Rotational Population (a.u.) - 250 nm	SD($v=0$) Rotational Population (a.u.) - 225 nm	SD($v=0$) Rotational Population (a.u.) - 223 nm
0	0.02	0.01	0.01
10	0.04	0.05	0.08
20	0.06	0.14	0.18
50	0.12	0.21	0.26
100	0.18	0.32	0.34
150	0.20	0.34	0.36
200	0.18	0.32	0.34
250	0.15	0.28	0.27
300	0.09	0.18	0.25
400	0.06	0.07	0.19
500	0.02	0.02	0.07
600	0.01	0.01	0.01
700	0.01	0.01	0.01

ter checking the signal rise time, choosing an appropriate photolysis wavelength, and employing the merged expansions to eliminate premixing of OCS and DI, we are confident that the observed RLDs are due to the reaction of D with OCS in a complex. The RLD obtained under these conditions is shown in Fig. 6. Note that the RLDs obtained under bulk and complexed conditions are essentially the same, i.e., quite cold, peaking at $\sim 180\text{ cm}^{-1}$. A comparison is presented in Fig. 7.

Bias in the Λ -doublet states is not detectable with the present experimental limits. Relative populations of the two spin-orbit states cannot be given since the upper state was not recorded due to low S/N. With complexes, $J \sim 10.5$ ($^2\Pi_{3/2}$) was the highest observed rotational state; under bulk conditions the highest observed J values are 14.5 ($^2\Pi_{3/2}$) and 5.5 ($^2\Pi_{1/2}$).



Rotational Energy / cm ⁻¹	R ₁₁ (□)	P ₁₁ (○)	Q ₁₁ (△)	Average (●)
0	0.05	0.05	0.05	0.05
20	0.10	0.15	0.10	0.12
40	0.25	0.30	0.25	0.28
60	0.58	0.50	0.35	0.48
80	0.85	0.80	0.48	0.72
100	1.00	0.95	0.80	0.92
120	0.98	0.80	0.78	0.95
140	0.68	0.65	0.78	0.65
160	0.30	0.30	0.58	0.40
180	0.30	0.10	0.35	0.18
200	0.10	0.05	0.20	0.08
220	0.05	0.02	0.05	0.05
240	0.02	0.01	0.02	0.02

FIG. 6. SD($v=0$) rotational distributions for complexes; 250 nm photolysis. Open squares, open triangles, and open circles are for R_{11} , Q_{11} , and P_{11} , respectively. Filled circles represent the average over these branches.

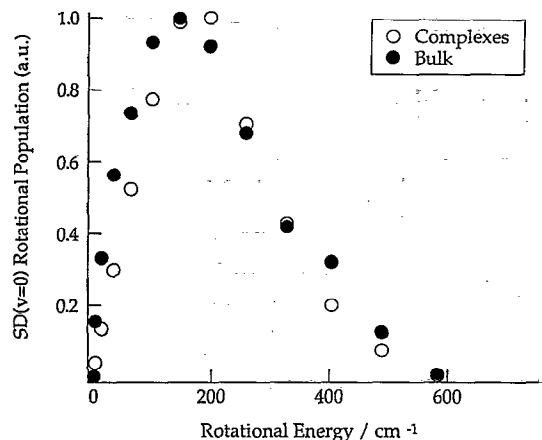


FIG. 7. SD($v=0$) rotational distributions for bulk and complexed conditions: 250 nm photolysis.

DISCUSSION

Experimentally, the H(D) + OCS system is well characterized. Every product except CS has been observed and E, V, R, T distributions have been measured for several photolysis wavelengths. Despite this, the reaction mechanism has yet to be established unambiguously. In the following discussion, possible mechanisms will be inferred from scrutiny of the experimental data and the recently available PES.^{24,25}

At this point, it seems reasonable to take a look at the present and previous data and at the mechanistic implications of those results. SD rotations are strikingly cold. A prior distribution³⁷ is sufficient to illustrate the large difference between the data and a statistical rotational distribution, as shown in Fig. 8. The prior peaks at $N \sim 30$ while the data peak at $N \sim 6$. This is a very large effect which clearly shows that statistical models of product state distributions are not applicable to this reaction. As stated above, our results are uncontaminated by secondary reac-

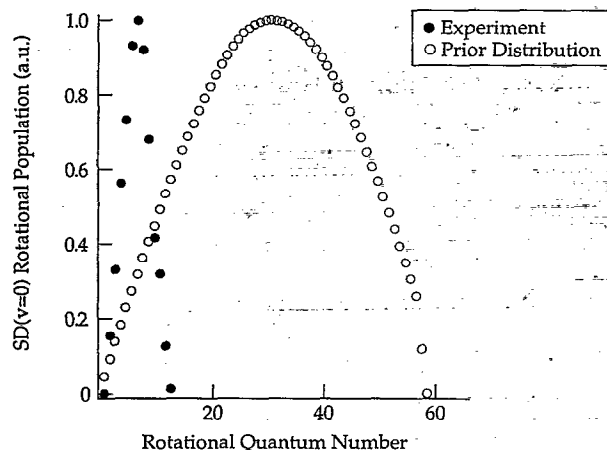


FIG. 8. SD($v=0$) rotational population as a function of quantum number. Dark circles show experimental results (250 nm photolysis, bulk conditions); open circles are a prior distribution.

tions that could give rotationally cold SD, the most likely of which is



where $S(^1D)$ is produced by OCS photodissociation. Because of the small absorption cross section at 250 nm ($4 \times 10^{-21} \text{ cm}^2$), OCS photodissociation is minimal.³⁸ Furthermore, distributions obtained at 223 and 225 nm are consistently the same as the one obtained at 250 nm. At these shorter wavelengths OCS *does* dissociate, but the absorption cross section is orders of magnitude smaller than that of DI.³⁸ Using 193 nm photolysis, Häusler *et al.* measured the SD concentration due to reaction (3) relative to the SD concentration due to the reaction of D atoms with OCS.³⁰ Even with DCI as a precursor, the fraction of SD caused by $S(^1D) + DCI$ was negligible.³⁰ We therefore believe that under our conditions rotational populations obtained at 223 and 225 nm reflect the reaction of D with OCS.

The SD rotational distribution obtained with complexes is very similar to that obtained under bulk conditions. We have taken severe precautions to prevent heterogeneous reaction of DI and OCS, as described in the experimental section. In addition, DI was photolyzed at 250 nm. Thus, we are confident that we were able to eliminate unwanted sources of SD, and that the RLDs shown in Figs. 6 and 7 reflect SD produced by the D + OCS reaction photoinitiated in complexes, with some contributions from higher-than-binary complexes. At first sight, the distribution seems to suggest that the reaction mechanism does not change when going from bulk conditions to complexes. This is not necessarily the case. In the H + N₂O system, the OH population measured with complexes is influenced by interactions with the nearby halogen atom.^{8,9,16} Such interactions cannot be excluded *a priori* for OCS-DI complexes.

Interestingly, for the high energy NH + NO channel of the H + N₂O system, NH rotational distributions are slightly colder with complexes than under bulk conditions, though both distributions are qualitatively similar. This was attributed in part to the squeezed atom effect.^{2,3,23,25,26,39} The OD rotational distributions of the high energy CS + OD channel are similar for bulk and complexed conditions and do not reflect a squeezed atom effect (see Figs. 9 and 10).³⁰ Since the excess energy is small (1670 cm^{-1}) the near-statistical OD rotational distribution is not surprising. Specifically, Rice *et al.* attribute this to a weakly bound linear ODCS species (structure *i* in Fig. 1).²⁴ Under the present conditions, rotational cooling attributable to the squeezed atom effect might be outside our resolution, i.e., modest S/N makes conclusions based on the OD distribution obtained with complexes unwarranted.

Studies of the CO product can further help to establish the reaction mechanism, since predissociation of SD $A^2\Sigma$ levels precludes the possibility of a full characterization of SD internal energy states, namely, making it impractical to obtain relative populations for the higher vibrational levels. Nascent CO was found to be colder rotationally and vibrationally than was predicted on statistical grounds, with energy preferentially channeled into c.m. translation.²⁵ The

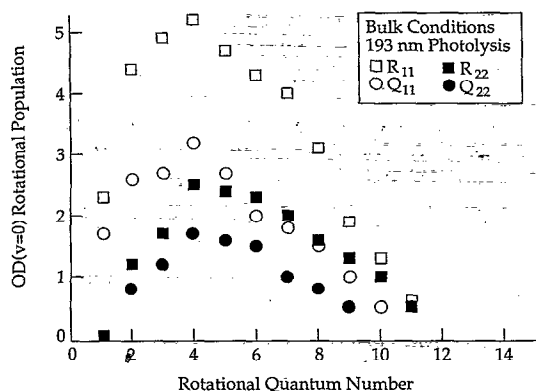


FIG. 9. OD($v=0$) rotational distribution; bulk conditions; 193 nm photolysis. Open squares and circles represent R_{11} and Q_{11} transitions, respectively. Dark squares and circles represent R_{22} and Q_{22} transitions, respectively.

authors also carried out a Franck-Condon analysis of CO vibrations based on a sudden change of the C-O bond length from that in OCS to that of free CO.²⁵ The measured CO vibrational distribution was slightly hotter than the calculated distribution.

All results point to a very short lived DSCO reaction intermediate. However, the question remains: Does deuterium attach initially to the oxygen, the carbon, or the sulfur? If it attaches initially to the oxygen and subsequently migrates to the sulfur, the CO will probably be vibrationally excited unless there is a significant local minimum for the HCOS structure. For example, note that the 1,3-hydrogen shift, $\text{HNNO} \rightarrow \text{NNOH} \rightarrow \text{N}_2 + \text{OH}$, leaves the N_2 with $\sim 20\,000\text{ cm}^{-1}$ of vibrational energy.²³

The CO deriving from reaction (2) is in no way similar to the N_2 from the $\text{H} + \text{N}_2\text{O}$ reaction—it even has slightly less vibrational excitation than predicted on statistical grounds. Alternatively, hydrogen attachment to the sulfur need not change the CO bond length significantly. Consequently, we calculated Franck-Condon factors for different C-O lengths projected onto free CO, as shown in Fig. 11. The measured CO vibrational distribution decreases monotonically, which is best reflected by Franck-Condon

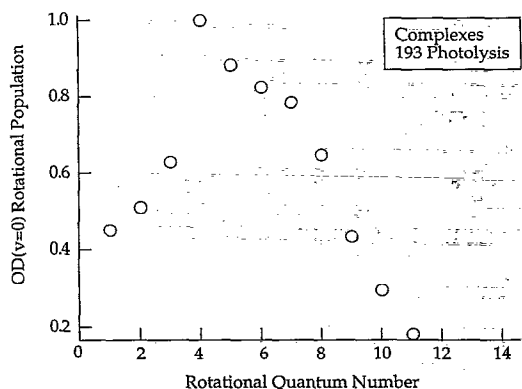


FIG. 10. OD($v=0$) rotational distribution; OCS-DBr complexes; 193 nm photolysis.

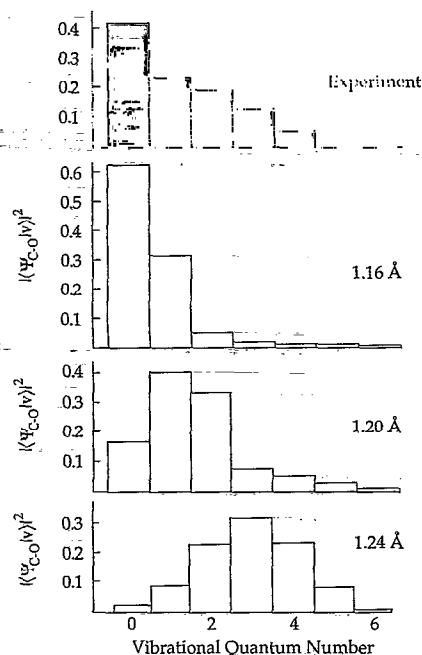


FIG. 11. Bar graphs of the experimental vibrational population and calculated Franck-Condon factors $|\Psi_{\text{C-O}}|v|^2$ vs vibrational quantum number. Shaded bars correspond to the experimental CO vibrational distribution (Ref. 27). Unshaded bars correspond to mean C-O separations of 1.16, 1.20, and 1.24 Å, respectively.

factors that use a C-O length close to that in OCS. Small differences are easily accounted for by the crudeness of the assumptions made in the calculation. The experimental findings cannot be reconciled with the substantial CO bond lengthening expected for a *rapid* 1,3 shift mechanism analogous to that found in the $\text{H} + \text{N}_2\text{O}$ system. They are consistent with the C-O length not changing much from that in OCS. On the basis of these considerations, we deduce that deuterium attacks sulfur directly and/or that the transient DCOS species is the immediate precursor of short-lived DSCO.²⁴

For direct deuterium attack at the sulfur, does reaction favor broadside or end-on approaches? To discuss this point, we refer to Fig. 12 for $\text{H} + \text{CO}_2$, which shows π orbital and nonbonding oxygen orbitals. For end-on attack the hydrogen 1s orbital overlaps with the nonbonding orbital from the oxygen, which has predominant s character. This interaction is repulsive.¹⁶ For broadside attack, the hydrogen orbital overlaps with the π orbitals of the CO double bond. This $s-\pi$ interaction is the only one known to react.¹⁶ Since the same qualitative considerations are expected to apply for $\text{H} + \text{OCS}$, we conclude that deuterium will react from broadside approaches, and we anticipate a relatively small reaction probability for end-on approaches. Figure 13 shows calculated geometries for the transition states which lead to *cis*- and *trans*-HSCO, taken from the work of Rice *et al.*²⁴ These structures support the premise that broadside approaches are reactive.

Recently, the structure of HBr-OCS has been measured by using high resolution spectroscopy. It was found to be quasilinear, with the hydrogen believed bonded to the

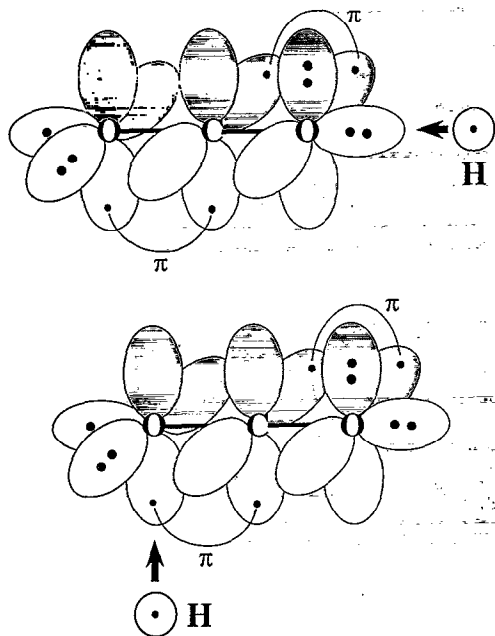


FIG. 12. CO₂ valence orbitals. (a) End-on hydrogen approach is repelled by nonbonding oxygen orbitals. (b) Broadside hydrogen approach results in reactive overlap with an oxygen π orbital.

oxygen.⁴⁰ Though reasonable, this was unanticipated, since both CO₂-HBr and N₂O-HBr are inertially T shaped.^{15-17,41,42} It will be important to measure the HI-OCS structure. Hopefully, a useful comparison can then be made between photoinitiated reactions in HBr-OCS and HI-OCS complexes.

Reaction via the SD+CO channel proceeds at energies that are well above any well depths along this reaction coordinate. Thus, it is likely that the dynamics do not reflect the equilibrium features of the PES. For reaction to take place at all, the incident deuterium must be slowed considerably. However, once the C-S interaction is repulsive, the rotational distribution in SD will mirror the an-

isotropy of the repulsive exit channel interaction.³⁰ In the case of D+OCS, exit channel repulsion will not put torque on SD because the c.m. sits essentially on the sulfur. The anisotropy of the repulsive interaction is probably small, and the resulting SD rotations are cold. The experimental findings for the cluster experiments suggest that the mechanism does not change, but it is not possible to discuss this issue with certainty before the interactions of SD with the nearby halogen atom have been clarified.

CONCLUSIONS

The SD($v=0$) rotational distributions obtained from reaction (2) under bulk conditions and with complexes have been found to be very cold; they peak near $N=6$, while on statistical grounds they are expected to peak near $N=30$. Furthermore, the distributions are essentially the same with complexes and under bulk conditions, suggesting the possibility of a common mechanism.

The OD rotational distributions from the high energy CS+OD channel are similar under bulk and complexed conditions. Little excess energy is available over the endothermicity of this channel. No marked squeezed atom effect was observed, but modest S/N precludes further interpretation.

The measured CO vibrational distribution²⁵ cannot be reconciled with the substantial CO bond lengthening expected for a rapid 1,3-hydrogen shift mechanism, such as the one observed for the OH+N₂ channel in the H+N₂O system. On the contrary, the CO vibrational distribution decreases monotonically and is even slightly colder than statistical predictions. Based on the fact that the measured vibrational distribution is best reflected by Franck-Condon factors for a CO-O length that is slightly longer than the equilibrium bond length of CO in OCS, we conclude that under bulk conditions deuterium either attacks the sulfur directly or gets to the sulfur via the HCOS intermediate. Specifically, there is not a rapid 1,3-hydrogen shift from the oxygen to the sulfur. The H+OCS system differs from the H+CO₂ and H+N₂O systems in an important way; the HCOs structure is relatively stable, as reported in the recent theoretical study of Rice, Cartland, and Chabalowski.²⁴

Under bulk conditions, we argue by analogy with the isovalent H+CO₂ system that deuterium attack of sulfur from an end-on approach is unfavorable compared to attack from the side. Specifically, in end-on approaches the hydrogen 1s orbital interacts with a nonbonding sulfur orbital, and this interaction is most likely repulsive. On the other hand, we believe that interactions of the 1s orbital with the π orbitals of the CS double bond are reactive. It is also possible for reaction to proceed via HCOS, in which case there is no counterpart in the H+CO₂ and H+N₂O systems.

With complexes, we point out the recent measurements of Hu, Chappell, and Sharpe,⁴⁰ in which a quasilinear BrH-OCS structure is reported. In itself, this is a major finding, as it impacts our understanding of the qualitative differences that can occur with isovalent moieties in weakly bound systems. The BrH-OCS complex is expected to be

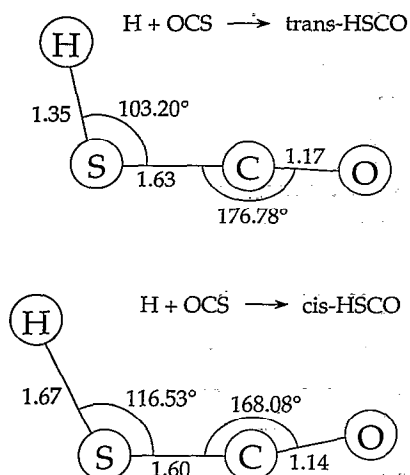


FIG. 13. Geometry of transition structures leading to *cis*- and *trans*-HSCO, respectively (Ref. 24). Bond lengths are given in Å.

very floppy. This structure is consistent with observations made with photoexcited OCS–HBr complexes. (i) The OH+CS channel is open under complexed conditions. If the sulfur were attacked directly, it is hard to imagine the hydrogen making its way to the oxygen.

(ii) The SH rotational distributions are similar under bulk and complexed conditions, which is consistent with minimal interaction of SH with the halogen. It will be important to measure the OCS–HI structure, since this can provide the basis for a valuable comparison between photoinitiated reactions in OCS–HBr vs OCS–HI complexes.⁴³ With BrH–OCS complexes, the SH+CO channel is most likely accessed via HCOS.

All of the experimental results suggest that DSCO is very short lived. Reaction (2) proceeds far above the wells and barriers in the exit channel region, and therefore it is unlikely that product excitations reflect the equilibrium properties of the PES. Deuterium must be slowed considerably for reaction to occur, and SD rotational distributions reflect a small anisotropy of the exit channel interaction. Finally, we note that femtosecond resolution studies of this system can assist greatly in establishing the mechanism in complexes.

ACKNOWLEDGMENTS

The authors received valuable inputs from B. M. Rice, H. E. Cartland, and C. F. Chabalowski, who calculated the PES used in our discussion. We thank S. W. Sharpe for communicating his group's results (Ref. 40) prior to publication. We are pleased to acknowledge many fruitful discussions with the above authors as well as S. L. Nickolaisen and R. A. Beaudet. Research supported by the U. S. Department of Energy under Contract No. DE-FG03-85ER13363.

- ¹S. Buelow, G. Radhakrishnan, J. Catanzarite, and C. Wittig, *J. Chem. Phys.* **83**, 444 (1985).
- ²G. Radhakrishnan, S. Buelow, and C. Wittig, *J. Chem. Phys.* **84**, 727 (1986).
- ³S. Buelow, M. Noble, G. Radhakrishnan, H. Reisler, C. Wittig, and G. Hancock, *J. Phys. Chem.* **90**, 1015 (1986).
- ⁴S. Buelow, G. Radhakrishnan, and C. Wittig, *J. Phys. Chem.* **91**, 5409 (1987).
- ⁵N. F. Scherer, L. R. Khundkar, R. B. Bernstein, and A. H. Zewail, *J. Chem. Phys.* **87**, 1451 (1987).
- ⁶J. Rice, G. Hoffmann, and C. Wittig, *J. Chem. Phys.* **88**, 2841 (1988).
- ⁷C. Wittig, Y. M. Engel, and R. D. Levine, *Chem. Phys. Lett.* **153**, 411 (1988).
- ⁸Y. Chen, G. Hoffmann, and C. Wittig, *J. Chem. Soc. Faraday Trans. II* **85**, 1292 (1989).
- ⁹Y. Chen, G. Hoffmann, D. Oh, and C. Wittig, *Chem. Phys. Lett.* **159**, 426 (1989).
- ¹⁰G. Hoffmann, D. Oh, Y. Chen, Y. M. Engel, and C. Wittig, *Isr. J. Chem.* **30**, 115 (1990).
- ¹¹T. Rose, M. J. Rosker, and A. H. Zewail, *J. Chem. Phys.* **91**, 7415 (1989).
- ¹²M. Dantus, R. M. Bowman, M. Gruebele, and A. H. Zewail, *J. Chem. Phys.* **91**, 7437 (1989).
- ¹³N. F. Scherer, C. Sipes, R. B. Bernstein, and A. H. Zewail, *J. Chem. Phys.* **92**, 5239 (1990).
- ¹⁴S. K. Shin, Y. Chen, D. Oh, and C. Wittig, *Philos. Trans. R. Soc. London Ser. A* **332**, 362 (1990).
- ¹⁵S. K. Shin, Y. Chen, S. Nickolaisen, S. W. Sharpe, R. A. Beaudet, and C. Wittig, *Adv. Photochem.* **16**, 249 (1991).
- ¹⁶(a) S. K. Shin, C. Wittig, and W. A. Goddard III, *J. Phys. Chem.* **95**, 5723 (1991). (b) Y. Chen, G. Hoffmann, S. K. Shin, D. Oh, S. W. Sharpe, Y. P. Zeng, R. A. Beaudet, and C. Wittig, in *Advances in Molecular Vibrations and Collision Dynamics*, edited by J. M. Bowman (JAI, Greenwich, 1991), p. 187.
- ¹⁷S. K. Shin, Y. Chen, E. Böhmer, and C. Wittig, in *Regioselective Photochemistry in Weakly Bonded Complexes*, in *The Dye Laser: 20 Years*, edited by M. Stuke, Topics in Applied Physics (Springer-Verlag, Berlin, 1992), Vol. 70, p. 57.
- ¹⁸S. I. Ionov, G. A. Brucker, C. Jaques, L. Valchovic, and C. Wittig, *J. Chem. Phys.* **97**, 9486 (1992).
- ¹⁹S. P. Walch, *J. Chem. Phys.* **98**, 1170 (1993).
- ²⁰G. Hoffmann, D. Oh, H. Iams, and C. Wittig, *Chem. Phys. Lett.* **155**, 356 (1989).
- ²¹G. Hoffmann, D. Oh, and C. Wittig, *J. Chem. Soc. Faraday Trans. II* **85**, 1141 (1989).
- ²²H. Ohoyama, M. Takayanagi, T. Nishiyama, and I. Hanazaki, *Chem. Phys. Lett.* **162**, 1 (1989).
- ²³E. Böhmer, S. K. Shin, Y. Chen, and C. Wittig, *J. Chem. Phys.* **97**, 2536 (1992).
- ²⁴B. M. Rice, H. E. Cartland, and C. F. Chabalowski, *Chem. Phys. Lett.* **211**, 283 (1993).
- ²⁵S. L. Nickolaisen and H. E. Cartland, *J. Chem. Phys.* **99**, 1145 (1993).
- ²⁶G. A. Oldershaw and D. A. Porter, *J. Chem. Soc. Faraday Trans. I* **68**, 709 (1972).
- ²⁷S. Tsunashina, T. Yokota, I. Safarik, H. E. Gunning, and O. P. Strausz, *J. Phys. Chem.* **79**, 775 (1975).
- ²⁸J. H. Lee, L. J. Stief, and R. B. Timmons, *J. Chem. Phys.* **67**, 1705 (1977).
- ²⁹G. A. Oldershaw and A. Smith, *J. Chem. Soc. Faraday Trans. I* **74**, 1687 (1978).
- ³⁰D. Häusler, J. Rice, and C. Wittig, *J. Chem. Phys.* **91**, 5413 (1987).
- ³¹J. J. Tice, M. J. Ferris, and F. B. Wampler, *J. Chem. Phys.* **79**, 130 (1983).
- ³²R. R. Friedl, W. H. Brune, and J. G. Anderson, *J. Chem. Phys.* **79**, 4227 (1983).
- ³³M. Kawasaki, H. Sato, G. Inoue, and M. Suzuki, *J. Chem. Phys.* **91**, 6758 (1989).
- ³⁴D. Ramsay, *J. Chem. Phys.* **20**, 1920 (1952).
- ³⁵C. M. Pathak and H. B. Palmer, *J. Mol. Spectrosc.* **32**, 157 (1969).
- ³⁶B. R. Weiner, H. B. Levenc, J. J. Valentini, and A. P. Baronavski, *J. Chem. Phys.* **90**, 1403 (1989).
- ³⁷R. D. Levine and R. B. Bernstein, *Molecular Reaction Dynamics and Chemistry Reactivity* (Oxford, New York, 1987).
- ³⁸H. Okabe, *Photochemistry of Small Molecules* (Wiley, New York, 1978).
- ³⁹R. D. Levine and J. L. Kinsey, in *Atom-Molecule Collision Theory*, edited by R. B. Bernstein (Plenum, New York, 1979), p. 693.
- ⁴⁰T. A. Hu, E. L. Chappell, and S. W. Sharpe (unpublished).
- ⁴¹S. W. Sharpe, Y. P. Zeng, C. Wittig, and R. A. Beaudet, *J. Chem. Phys.* **92**, 943 (1990).
- ⁴²Y. P. Zeng, S. W. Sharpe, D. Reifschneider, C. Wittig, and R. A. Beaudet, *J. Chem. Phys.* **93**, 183 (1990).
- ⁴³S. W. Sharpe (private communication).